

## Pressure Tuning between $\text{NH}\cdots\text{N}$ Hydrogen-Bonded Ice Analogue and $\text{NH}\cdots\text{Br}$ Polar dabcoHBr Complexes

Armand Budzianowski and Andrzej Katrusiak\*

Faculty of Chemistry, Adam Mickiewicz University, Grunwaldzka 6, 60-780 Poznań, Poland

Received: February 27, 2006; In Final Form: March 30, 2006

At normal conditions 1,4-diazabicyclo[2.2.2]octane hydrobromide  $[\text{C}_6\text{H}_{13}\text{N}_2]^+\text{Br}^-$  forms centrosymmetric crystals, space group  $P6m2$ ,  $\text{NH}^+\cdots\text{N}$  hydrogen-bonded linear polycationic chains with disordered protons in the structure. As in  $\text{H}_2\text{O}$  ice *Ih*, the protons in  $[\text{C}_6\text{H}_{13}\text{N}_2]^+\text{Br}^-$  crystals remain disordered at low temperatures. Above 0.4 GPa the  $[\text{C}_6\text{H}_{13}\text{N}_2]^+\text{Br}^-$  crystals transform into a new polar  $\text{NH}^+\cdots\text{Br}^-$  hydrogen bonded complex, space group  $Cmc2$ . It has been crystallized in-situ in a diamond anvil cell and its structure determined by X-rays. The low-pressure triggering of this transformation indicates that it is a possible source of defects in the real structure at normal conditions, where, along with disproportionation defects, they can be responsible for anomalous dielectric properties, including relaxor-like behavior of  $\text{NH}\cdots\text{N}$  hydrogen-bonded compounds.

While hydrogen bonds are abundant in nature and play a fundamental role for properties of many natural (mineral) and synthetic (e.g., pharmacological) substances and all biological species,<sup>1</sup> there are no commercial electronic devices based on H-bonded materials. Recently, ferroelectric properties coupled to the proton dynamics were detected in the  $\text{NH}^+\cdots\text{N}$  hydrogen-bonded ionic complexes of 1,4-diazabicyclo[2.2.2]octane (denoted dabco), in certain respects analogous to well-known  $\text{OH}\cdots\text{O}$  bonded ferroelectrics.<sup>2,3</sup> The spontaneous polarization of these  $\text{NH}^+\cdots\text{N}$  bonded salts can be much higher than in most known ferroelectrics. Also relaxor-like behavior was observed in the dabco monosalts, where polar nanodomains are formed within the matrix structure.<sup>4</sup> It was shown that the dabco $\text{H}^+$  cations in the dabcoHA monosalts (HA stands for HBr,  $\text{HClO}_4$ ,  $\text{HBF}_4$ ,  $\text{HReO}_4$ ) are linked into linear polycationic chains by  $\text{NH}^+\cdots\text{N}$  bonds, and that the protons become disordered in two sites in the paraelectric phase above  $T_c$ .<sup>2,5</sup> The observations of nanodomains and relaxor-like behavior imply that the crystal is capable of transforming its regions into other structures, which generate new dielectric bulk properties. For example, seemingly centrosymmetric crystals can exhibit a strong dielectric response, resulting from highly polarized microregions. In materials built of linear bistable  $\text{NH}^+\cdots\text{N}$  bonded chains, such regions may be generated by defects of  $\text{NH}^+\cdots\text{N}$  or  $\text{N}\cdots\text{H}^+\text{N}$  arrangements, reversing chain polarity.<sup>4,6</sup>

In this paper we demonstrate, that the polycationic H-bonded chains of dabcoHBr<sup>6</sup> can be transformed into a quite different structure of H-bonded cations and anions by modest pressure of about 0.4 GPa. Such highly polar nanoregions built of H-bonded dabco $\text{H}^+\cdots\text{Br}^-$  pairs can drastically change the dielectric properties of the substance. The thermodynamic work term (i.e., the work of compressing the crystal to the volume, when the transformation is triggered) implied by the pressure

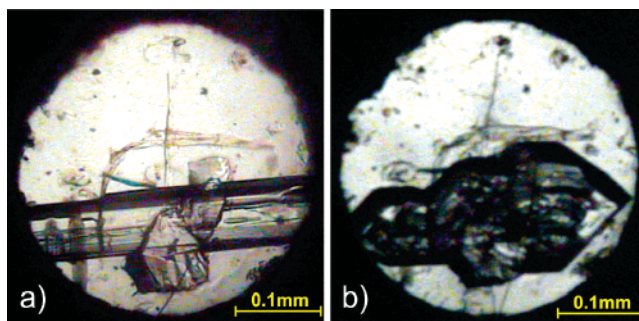


**Figure 1.** Single crystals of dabcoHBr in equilibrium with solvent in the high-pressure chamber: (a) phase  $\alpha$  at 0.30 GPa, and (b) phase  $\beta$  at 0.78 GPa, both at 296 K. Two ruby chips for pressure calibration lie below and above the middle section of the sample crystal.

range investigated is equivalent to, or smaller than, the energy of intermolecular interactions in crystals.

The effects of pressure on the dabcoHBr structure have been studied by X-ray diffraction in a Merrill–Bassett diamond-anvil cell (DAC).<sup>7</sup> Our initial studies on a single crystal mounted in the DAC failed due to destructive transformations of the sample. Therefore, instead of performing the experiments on single-crystal samples mounted in the DAC at ambient conditions and then compressed to the required pressure, dabcoHBr was crystallized in-situ from the methanol solution in the DAC, using a procedure similar to that described by Fabiani et al.<sup>8</sup> To enhance the performance of this method we loaded the DAC with grains of dabcoHBr and its saturated methanol solution. The pressure was calibrated using the ruby  $R_1$ -fluorescence technique<sup>9</sup> and a BETSA PRL spectrometer. At 0.30 GPa, all crystals but one were dissolved by increasing temperature to 370 K. Slow cooling allowed this one grain to grow. Owing to the large volume of so-obtained single crystals (Figure 1a) and an optimized data collection procedure,<sup>10</sup> we could measure the reflection intensities on a laboratory KUMA KM4-CCD diffractometer equipped with a sealed X-ray tube.

\* Corresponding author. Telephone: +48(61)8291443. Fax: +48(61)-8658008. E-mail: katran@amu.edu.pl

**TABLE 1: Crystal Data and Experimental Details for dabcoHBr at 0.1 MPa and at 0.30 and 0.78 GPa, All at 296(1) K<sup>14</sup>**

	phase $\alpha$		phase $\beta$
pressure (GPa)	0.0001	0.30(5)	0.78(5)
space group	$P6m2$	$P6m2$	$Cmc2_1$
$a$ (Å)	6.673(1)	6.604(2)	7.373(2)
$b$ (Å)	6.673(1)	6.604(2)	10.212(6)
$c$ (Å)	5.331(1)	5.256(2)	9.855(5)
$V$ (Å <sup>3</sup> )	205.59(9)	198.54(10)	742.0(6)
$Z$	1	1	4
$D_x$ (g·cm <sup>-3</sup> )	1.560	1.615	1.728
$R_1[F^2 > 2\sigma(F^2)]$	0.026	0.086	0.038
GoF	1.02	1.06	1.01

**TABLE 2: Atomic Coordinates ( $\times 10^4$ ) and Equivalent Isotropic Displacement Parameters (Å<sup>2</sup>  $\times 10^3$ ) for dabcoHBr at 0.3 GPa<sup>a</sup>**

	$x$	$y$	$z$	$U(\text{eq})^a$
Br	0	0	0	13(1)
N(1)	3333	6667	2660(50)	49(10)
C(1)	4520(30)	9040(50)	3520(30)	50(6)
H(N)	3333	6667	931	59
H(C)	3731	9844	2889	60

<sup>a</sup>  $U(\text{eq})$  is defined as one-third of the trace of the orthogonalized  $U_{ij}$  tensor.

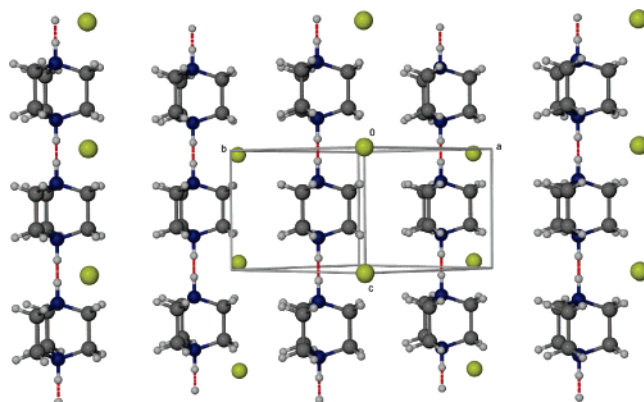
**TABLE 3: Atomic Coordinates ( $\times 10^4$ ) and Equivalent Isotropic Displacement Parameters (Å<sup>2</sup>  $\times 10^3$ ) for dabcoHBr at 0.78 GPa<sup>a</sup>**

	$x$	$y$	$z$	$U(\text{eq})^a$
Br(1)	0	4414(1)	6560(3)	33(1)
N(1)	0	7341(8)	5445(11)	30(2)
N(2)	0	9421(7)	4069(11)	32(2)
C(1)	-1669(8)	7374(7)	4559(10)	30(2)
C(2)	-1627(11)	8640(8)	3727(12)	38(2)
C(3)	0	8465(8)	6420(20)	38(2)
C(4)	0	9720(12)	5507(18)	42(3)
H(N)	0	6580	5926	290(170)
H(1A)	-2780(80)	7320(70)	5120(90)	36
H(1B)	-1810(90)	6560(70)	3880(100)	36
H(2A)	-1330(110)	8490(80)	3050(120)	45
H(2B)	-2670(100)	9120(80)	4060(80)	45
H(3A)	1110(80)	8380(70)	6900(110)	45
H(4A)	-980(100)	10160(80)	5560(100)	50

<sup>a</sup>  $U(\text{eq})$  is defined as one-third of the trace of the orthogonalized  $U_{ij}$  tensor.

After applying accurate analytical corrections ( $40 \times 40 \times 20$  divisions across the high-pressure chamber and along the DAC axis, respectively) for the absorption of the sample, absorption of the DAC, and gasket shadowing,<sup>11</sup> the structure was solved straightforwardly by direct methods<sup>12–14</sup> and shown to correspond to the ambient pressure phase (cf. Table 1). When the pressure was increased to 0.78 GPa, the needle-like crystal grown at 0.30 GPa crushed and started to dissolve at room temperature, while new prismatic crystals appeared. The crushed fragments dissolved slowly and changed their shape into the prismatic one, after which they resumed growing in the new morphology. The new crystals initially grew from solution, and later at the cost of the crushed sample. Again, the DAC was heated until all but one crystal melted at 385 K, after which the DAC was slowly cooled, allowing this one grain to grow until 296 K. Its crystal habit was clearly different from that at 0.30 GPa (Figure 1b). The X-ray diffraction measurement for the crystal at 0.78 GPa and its structure solution<sup>12,13</sup> were performed as described above.<sup>14</sup> The final atomic parameters in phases  $\alpha$  and  $\beta$  are listed in Tables 2 and 3, respectively.

The crystal data, summarized in Table 1, revealed a new phase of dabcoHBr at 0.78 GPa, of different unit-cell shape and

**Figure 2.** Autostereographic<sup>16</sup> projection of  $\alpha$ -dabcoHBr structure at 0.30 GPa viewed along  $[110]_\alpha$ . The hydrogen bonds are shown as red dashed lines between the half-occupied sites of disordered protons.<sup>17</sup>

symmetry than the ambient pressure one. It became apparent, that dabcoHBr undergoes a transformation between 0.30 and 0.78 GPa. Hereafter, the low- and high-pressure structures of dabcoHBr will be denoted as phases  $\alpha$  and  $\beta$ , respectively.

After completing the intensity measurements at 0.78 GPa, the unit-cell dimensions of the  $\beta$ -phase were remeasured at 0.78 and 0.70 GPa. When the DAC was opened, the single-crystal did not survive the pressure release and disintegrated into white powder. Its powder diffraction pattern was recorded and successfully indexed for the  $\alpha$  phase. By continuing in-situ freezing of phases  $\alpha$  and  $\beta$  in the DAC, it was confirmed that the transition is reversible and that the transition pressure at 296 K is close to 0.4 GPa. At 0.30 GPa, the crystal in phase  $\alpha$  (Figure 2) has been squeezed to 93.4% of its ambient-pressure volume,<sup>6</sup> but the protons remain disordered in  $\text{NH}^+ \cdots \text{N}$  bonds of polycationic chains and equidistant to three closest  $\text{Br}^-$  anions. The intermolecular  $\text{N} \cdots \text{N}$  distance of 2.80(2) Å observed at 0.30 GPa is consistent with the distance of 2.787(8) Å determined at 0.1 MPa, the slight lengthening being much smaller than the obtained accuracy.

No sign of the  $\alpha$ -to- $\beta$  transformation of dabcoHBr was detected by DSC and X-ray diffraction and the proton remained disordered to 87 K at ambient pressure. In this respect dabcoHBr can be considered as a one-dimensional  $\text{NH}^+ \cdots \text{N}$  bonded  $\text{H}_2\text{O}$  *Ih* ice analogue. It appears that in both these structures, dabcoHBr and  $\text{H}_2\text{O}$  ice *Ih* the persistence of the disorder of the protons involved in the hydrogen bonding is common to the lowest temperatures (to 87 K in dabcoHBr) due to the very weak coupling between the H-sites and the arrangements of the  $\text{NH} \cdots \text{N}$  and  $\text{OH} \cdots \text{O}$  hydrogen-bonded ions and molecules.<sup>15</sup>

The high-pressure  $\beta$  phase is built of  $\text{NH}^+ \cdots \text{Br}^-$  bonded ionic pairs (Figure 3). The  $\text{N}^+ \cdots \text{Br}^-$  distance is 3.19(2) Å. Thus pressure above 0.4 GPa modifies the chemical association in this H-bonded complex of dabcoHBr by favoring the heteronuclear  $\text{NH}^+ \cdots \text{Br}^-$  hydrogen bonds over the homonuclear  $\text{NH}^+ \cdots \text{N}$  bonds. This chemical transformation lowers the symmetry and considerably strains the structure (see Table 1), which shatters the single-crystal sample on the  $\alpha$ -to- $\beta$  phase transition. Hence the in-situ crystallization of the  $\beta$  phase had to be applied.

A common feature of structures  $\alpha$  and  $\beta$  of dabcoHBr is that the ions are located in special positions,  $D_{3h}$  below 0.4 GPa, and  $C_s$  above. Thus the ethylene groups are restricted by symmetry to be eclipsed, which suggests that their torsional distortions are easily coupled to the lattice-mode vibrations.<sup>18</sup>

The intriguing feature of the crystal lattices of phases  $\alpha$  and  $\beta$  is that in certain respects they resemble each other despite

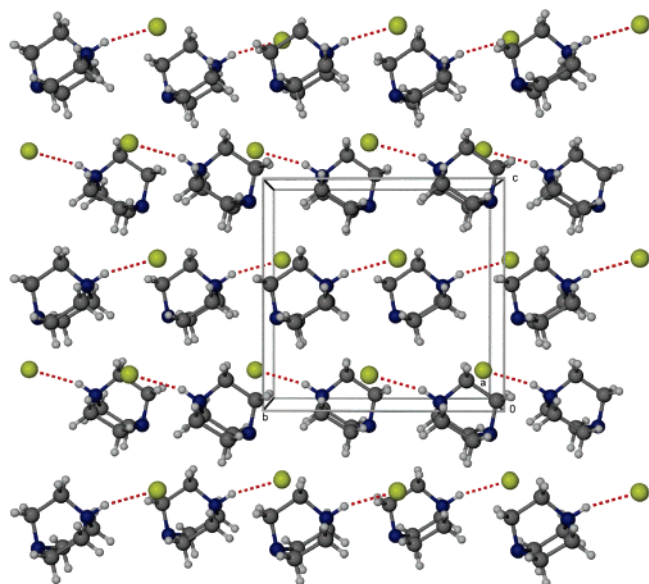


**Figure 3.** Autostereographic<sup>16</sup> projection of the  $\beta$ -dabcoHBr structure along  $[100]_{\beta}$  at 0.78(5) GPa. The hydrogen bonds have been shown as the red dashed lines.<sup>17</sup>

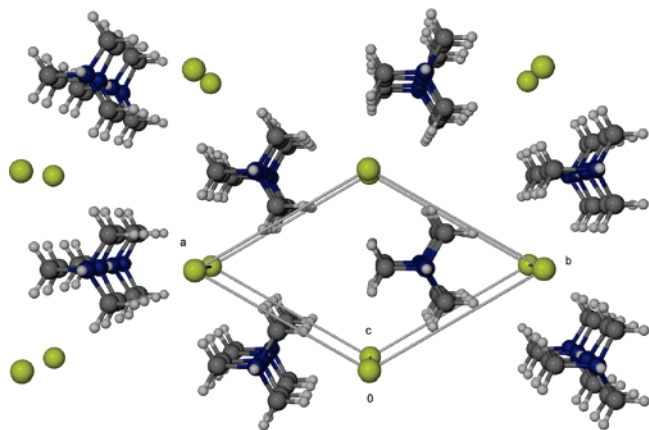


**Figure 4.** Autostereographic<sup>16</sup> projection of the  $\alpha$ -dabcoHBr structure at 0.30 GPa viewed down  $[001]_{\alpha}$  along the H-bonded chains.<sup>17</sup>

different chemical association of the ions in these structures. The transformation of the hexagonal cell of the  $\alpha$ -phase to the orthorhombic unit cell of the  $\beta$ -phase (compare Figures 4 and 5) can be represented by the matrix equation

$$\begin{pmatrix} a_{\beta} \\ b_{\beta} \\ c_{\beta} \end{pmatrix} = \tilde{S} \begin{pmatrix} 1 & 1 & 0 \\ -1 & 1 & 0 \\ 0 & 0 & 2 \end{pmatrix} \begin{pmatrix} a_{\alpha} \\ b_{\alpha} \\ c_{\alpha} \end{pmatrix} \quad (1)$$

The chemical transformation induces considerable strain in the structure. The strain tensor,  $\tilde{S}$ , calculated from the unit cell dimensions of the crystal in phase  $\alpha$  at 0.30 GPa and in phase  $\beta$  at 0.78 GPa (see Table 1) is

$$\tilde{S} = \begin{pmatrix} 1 + \epsilon_{11} & 0 & 0 \\ 0 & 1 + \epsilon_{22} & 0 \\ 0 & 0 & 1 + \epsilon_{33} \end{pmatrix} = \begin{pmatrix} 1.1164 & 0 & 0 \\ 0 & 0.8928 & 0 \\ 0 & 0 & 0.9375 \end{pmatrix} \quad (2)$$

where  $\epsilon_{ii}$  are anomalous strain components. The spontaneous

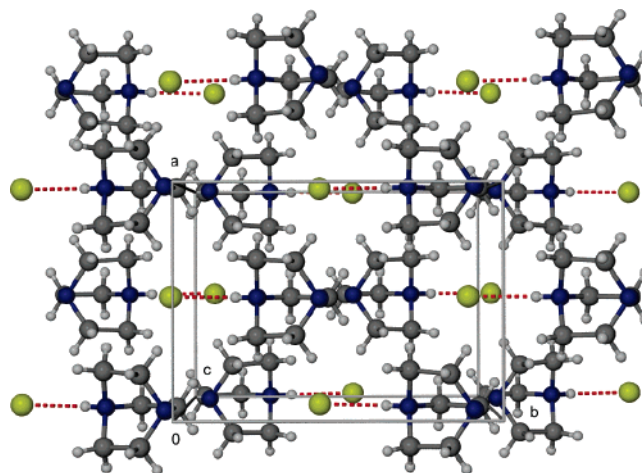


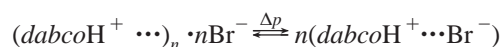
**Figure 5.** Autostereographic<sup>16</sup> projection of the  $\beta$ -dabcoHBr structure along  $[001]_{\beta}$  at 0.78(5) GPa. The hydrogen bonds  $\text{NH}^+ \cdots \text{Br}^-$  have been shown as the red dashed lines.<sup>17</sup>

shear strain in the form

$$e_{12} = \{(b_{\beta}/\sqrt{3} - a_{\beta})\}/\{(b_{\beta}/\sqrt{3} + a_{\beta})\}$$

can be employed as an order parameter describing this phase transition of the  $\bar{6}m2Fmm2$  species.<sup>19</sup> So defined ferroelastic shear strain  $e_{12} = 0.111$ , when calculated from the unit-cell dimensions at 0.30 and 0.78 GPa. This value illustrates the magnitude of strains generated in the dabcoHBr crystal when it transforms between phases  $\alpha$  and  $\beta$ . It is comparable in magnitude to the highest reported deformations of crystal phases, for example with those in 1,3-cyclohexanedione,<sup>20,21</sup> guanidinium nitrate,<sup>22,23</sup> and in  $\text{KHF}_2$  crystals.<sup>24</sup>

The group-subgroup symmetry relation between the dabcoHBr phases allows the  $\beta$  phase to be classified, at least formally, as a ferroelastic state of the prototypical phase  $\alpha$ . However, contrary to typical phase transitions, the transformations of dabcoHBr modify the H-bonded complexes according to the scheme



The molecular volume change associated with this transformation is  $1.77 \text{ \AA}^3$ . The average complex symmetry, centrosymmetric below 0.4 GPa and noncentrosymmetric and polar above (Table 1), is crucial for its dielectric properties. In the  $\beta$  phase the H-bonded ionic pairs (dipoles) are arranged in such a manner that their  $[z]$  components all have the same sense: all dabco cations in Figure 3 are located below the anions to which they are H-bonded. After the  $\text{NH}^+ \cdots \text{N}$  have been broken, the bulky cations had to move away from the previous axis of the chain, because the van der Waals interactions require more space for intermolecular contacts. Thus the cations shifted along the  $[010]_{\beta}$  direction and become inclined by  $57.4^\circ$  to the  $[001]_{\beta}$  axis (compare Figures 2–6). Somewhat smaller shifts, also preserving the mirror plane perpendicular to  $[100]_{\beta}$ , affected the positions of Br anions (Figures 3 and 5). In the  $\beta$  phase the hydrogen-bond dimensions are: distance  $\text{H}^+ \cdots \text{Br}^-$  2.34 Å and angle  $\text{NH}^+ \cdots \text{Br}^-$   $161.7^\circ$  (compared to the analogous non-H-bonding dimensions of 3.84 Å and  $97.3^\circ$  in the  $\alpha$  phase at 0.3 GPa, respectively).

The energy required for equalizing the thermodynamical potentials of phases  $\alpha$  and  $\beta$  can be assessed from the work performed on the crystal in phase  $\alpha$  by the external pressure (i.e., the integral  $\int \Delta V dp$  between ambient and transition



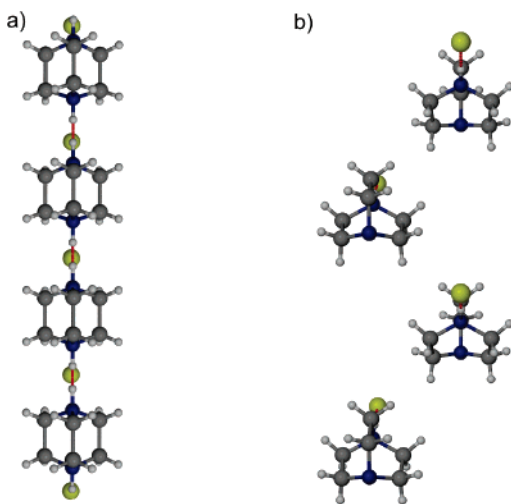


**Figure 6.** Projections of (a) one chain in the dabcoHBr at 0.3 GPa in phase  $\alpha$  viewed down  $[-110]_{\alpha}$ , and four H-bonded ionic pairs viewed along  $[010]_{\beta}$  in phase at 0.78(5) GPa. The hydrogen bonds have been shown as the red dashed lines.<sup>17</sup>

pressures). The energy triggering the transition estimated in this way is relatively small ( $E_p = 1.2$  kJ/mol) compared to the typical energy of lattice interactions in molecular and ionic crystals. Therefore nanosized regions of the  $\beta$ -form are likely to be created due to local-field stochastic pressure fluctuations in the  $\alpha$  form. Even short-range ferroelectric ordering in the polar  $\beta$  form could be also responsible for a relaxor-like behavior. The dielectric response observed for the hydrogen-bonded complex dabcoHBF<sub>4</sub> was associated with the formation of nanoregions induced by short-range ferroelectric ordering of the  $\text{NH}^+\cdots\text{N}$  hydrogen-bonds.<sup>5</sup> The evidenced transformation of dabcoHBr suggests that other structural mechanisms leading to short-range ferroelectric order are possible, e.g., changes of the H-bonding networks. The low energy required for triggering transformations of H-bonded complexes further suggests that isolated centers or nanoregions of different structure, modifying bulk properties of substances, can be common not only to the dabcoHA monosalts listed above but also to other H-bonded materials.<sup>4</sup>

**Acknowledgment.** Support from the Polish Committee for Scientific Research, Grant 3 T09A 131 26, is acknowledged.

## References and Notes

(1) (a) Jeffrey, G. A.; Saenger, W. *Hydrogen Bonding in Biological Structures*, Springer-Verlag: Berlin Heidelberg, 1991. (b) Nagle, J. F.; Mille,

- M.; Morovitz H. J. *J. Chem. Phys.* **1980**, *72*, 3959–3971. (c) Prewitt, Ch. T.; Parise, J. B. *Rev. Mineral. Geochem.* **2000**, *41*, 309–333.
- (2) (a) Katrusiak, A.; Szafranski, M. *Phys. Rev. Lett.* **1999**, *82*, 576–579. (b) Szafranski, M.; Katrusiak, A. *Phys. Rev. Lett.* **2002**, *89*, 2155071–4.
- (3) Katrusiak, A. *Phys. Rev. B* **1993**, *48*, 2992–3002.
- (4) Szafranski, M.; Katrusiak, A. *J. Phys. Chem. B* **2004**, 15709–15713.
- (5) Katrusiak, A. *J. Mol. Struct.* **2000**, *552*, 159–164.
- (6) Katrusiak, A.; Ratajczak-Sitarz, M.; Grech, E. *J. Mol. Struct.* **1999**, *474*, 135–141.
- (7) Merrill, L.; Bassett, W. A. *Rev. Sci. Instrum.* **1974**, *45*, 290–294.
- (8) Fabiani, F. P. A.; Allan, D. R.; David, W. I. F.; Moggach, S. A.; Parsons, S.; Pulham, C. R. *Cryst. Eng. Commun.* **2004**, *6*, 504–511.
- (9) (a) Piermarini, G. J.; Block, S.; Barnett, J. D.; Forman, R. A. *J. Appl. Phys.* **1975**, *46*, 2774–2780. (b) Mao, J. K.; Xu, J.; Bell, P. M. *J. Geophys. Res.* **1985**, *91*, 4673–4676.
- (10) Budzianowski, A.; Katrusiak, A. In *High-Pressure Crystallography*; Katrusiak, A., McMillan, P. F., Eds.; Kluwer Academic: Dordrecht, 2004; pp 157–168.
- (11) Katrusiak, A. *Z. Kristallogr.* **2004**, *219*, 461–467.
- (12) Sheldrick, G. M. *Acta Crystallogr.* **1990**, *A46*, 467–473.
- (13) Sheldrick, G. M. *The SHELX-97 manual*. University of Göttingen: Göttingen, Germany, 1997.
- (14) Both structures were refined by full-matrix least-squares: all non-H atoms were refined with anisotropic temperature factors for the structure  $\alpha$  at 0.30 GPa, and only Br was anisotropic in the structure  $\beta$  at 0.78 GPa. For the measurement at 0.30 GPa the carbon H-atoms were located from molecular geometry ( $d_{\text{C-H}}$  0.97 Å) after each cycle of the refinement and their  $U_{\text{iso}}$ 's were assumed as 1.2  $U_{\text{eq}}$ 's of their carriers. In the experiment at 0.78 GPa the hydrogen atoms were located from difference Fourier maps and refined with  $U_{\text{iso}}$ 's equal to 1.2  $U_{\text{eq}}$ 's of the carbon atoms. The acidic protons were located in the difference Fourier maps; however, the accuracy of their refined positions was low, therefore, in the final cycles of refinement their positions were determined from the idealized molecular geometry ( $d_{\text{N-H}}$  0.91 Å) with  $U_{\text{iso}}$ 's assumed as 1.2  $U_{\text{eq}}$ 's of their carriers. The Cambridge Crystallographic Data Centre contains the supplementary crystallographic data for phase  $\alpha$  at 0.30 GPa and phase  $\beta$  at 0.78 GPa in crystallographic information files (CIF format) CCDC 277833 and CCDC 277834, respectively, which can be obtained free of charge via [http://www.ccdc.cam.ac.uk/data\\_request/cif](http://www.ccdc.cam.ac.uk/data_request/cif).
- (15) (a) Katrusiak, A. *J. Mol. Struct.* **1999**, *474*, 125–133. (b) Katrusiak, A. *Phys. Rev. Lett.* **1996**, *77*, 4366–4369.
- (16) Katrusiak, A. *J. Mol. Graph. Model.* **2001**, *19*, 363–367, 398.
- (17) (a) Barbour, L. J. *J. Supramol. Chem.* **2001**, *1*, 189–191. (b) Atwood, J. L.; Barbour, L. J. *Cryst. Growth Des.* **2003**, *3*, 3–8. (c) <http://www.povray.org>.
- (18) Żogał, O. J.; Galewski, Z.; Grech, E.; Malarski, Z. *Mol. Phys.* **1985**, *56*, 47–53.
- (19) Aizu, K. *J. Phys. Soc. Jpn.* **1970**, *28*, 706–716.
- (20) Katrusiak, A. *Acta Crystallogr.* **1990**, *B46*, 246–256.
- (21) Katrusiak, A. *Acta Crystallogr.* **1991**, *B47*, 398–404.
- (22) Szafranski, M. *Solid State Commun.* **1992**, *84*, 1051–1054.
- (23) Katrusiak, A.; Szafranski, M. *J. Mol. Struct.* **1996**, *378*, 205–223.
- (24) Fink, R. W.; Westrum, E. F., Jr. *J. Phys. Chem.* **1956**, *60*, 800–801.